SCIENTIFIC PAPER

Development of a Breathable Polymeric Membrane and Process Optimization by Using a General Full Factorial Design

Imene Ghezal[1,2*], Ali Moussa[1,2], Imed Ben Marzoug[1,3], Ahmida El-Achari[4,5], Christine Campagne[4,5] And Faouzi Sakli[1,3]

[1] Textile Engineering Laboratory, *University of Monastir, 5070 Ksar-Hellal, Tunisia*

[2] *National Engineering School of Monastir, University of Monastir, 5019 Monastir, Tunisia*

[3] *Higher Institute of Technological Studies of Ksar-Hellal, 5070 Ksar-Hellal, Tunisia*

[4]*Université Lille Nord de France, 59000 Lille, France*

[5]*ENSAIT, GEMTEX, 2 Allée Louise et Victor Champier 59100 Roubaix, France*

https://doi.org/10.2298/CICEQ240202017G

Received 2.2.2024.

Revised 16.4.2024.

Accepted 8.5.2024.

[*] Corresponding author: Imene GHEZAL, Textile Engineering Laboratory, University of Monastir, 5070 Ksar-Hellal, Tunisia. Email: elghezalimene@hotmail.com, Telephone number: +216 94 836 791

Abstract

The aim of this research was to produce a breathable hydrophilic membrane that can be laminated to textile fabrics to enhance their resistance to water penetration without restricting their breathability. For this purpose, aliphatic polyester polyurethane and acrylic ester copolymers were used. Quantities of both chemicals were varied according to three levels each. A general full factorial design was used to analyze responses that were the water vapor permeability index (WVPI (%)) and the absorption rate (Abs rate (%)). The membrane synthesis process was then optimized by using the Minitab response optimizer. The optimum polymeric membrane water vapor permeability and absorption rate were equal to 504.148 $g \cdot m^{-2} \cdot day^{-1}$ and 50.401%, respectively. Based on obtained results, the developed polymeric membrane was judged breathable. The morphological aspect of the dense membrane was also analyzed. It was noticed that air bubbles with different morphological types appeared in the nonporous membrane structure. Finally, it was concluded that the developed membrane can be thermo-assembled with other textile layers to enhance their resistance to wind and water penetration without affecting their breathability.

Keywords: dense membrane, breathable membrane, absorption rate, water vapor permeability, windproofness.

Article highlights

- A hydrophilic membrane was produced with a knife on roller coating machine
- The membrane was mainly composed of aliphatic polyester polyurethane and acrylic ester copolymers
- Water vapor permeability index and absorption rate responses were analyzed
- The polymeric membrane formulation was optimized by using a general full factorial design
- The optimal membrane was judged breathable

Introduction

Traditional fabrics made with natural fibers are hygroscopic and non-durable [1]. On the other hand, synthetic fibers are not as breathable as natural ones [2]. The emerging of polymeric membranes took place to facilitate the production of materials that ensure protection and comfort to the wearer [3–8]. In the 1970s, the first waterproof breathable membranes were developed and then laminated to textiles. Since then, these materials were gaining interest due to their interesting properties such as their ability to protect the wearer against rain, wind, and snow while ensuring the evacuation of moisture vapor from the cloth inner side to the surrounded atmosphere [9,10].

The space between the wearer skin and the cloth is defined as the microclimate [2]. For wearer comfort, this microclimate should not be affected and the moisture between the skin and the cloth should be evacuated to the surrounded environment [2,11].

Waterproof breathable membranes can be used for producing directional water transport textile fabrics [12]. These membranes can be classified according to two categories: (a) microporous membranes and (b) hydrophilic ones [9,13]. For microporous membranes the water vapor transmission occurs through micropores. However, for hydrophilic ones the moisture vapor is transmitted from the inner side to the outer side by sorption, diffusion, and desorption processes [2]. The adsorption of water vapor by the membrane surface depends on the used polymer hydrophilicity and the material matrix free volume. Actually, water vapor molecules diffuse from the inner side to the outer side of the membrane by physico-chemical interactions between water vapor molecules and membrane hydrophilic sites. This migration depends on water vapor pressure and concentration, surrounding temperature, and humidity [2].

In the textile area, the most used polymers for membranes synthesis are polyurethanes, polytetrafluoroethylenes, acrylics, and poly(amino acids) [13–16]. Waterborne polyurethanes are mainly used for enhancing the resistance to water penetration of textiles [17]. They are mixed with acrylates in order to obtain enhanced hydrophobicity and water penetration resistance [17,18]. However, previously developed membranes present a poor breathability [19]. Added to that, used processes for producing these membranes are complicated and not easily applicable [6]. Generally, air permeability, water vapor permeability, and wettability are among the most tested properties for evaluating membranes comfort performance [20].

Recently, many researchers focused on the development of porous membranes. Zhou et al. [21] used electrospinning method for producing porous polyurethane based membranes. They found that developed structures exhibit desirable breathable performances [21]. In another study [22], polyamide and polydimethylsiloxane were both used for preparing nanofibrous membranes. The direct electrospinning technique was employed [22]. It was found that produced polymer material presented high breathability [22]. In a research conducted by Zhou et al. [23] heat treatment was applied to waterborne polyurethane membranes produced with emulsion electrospinning [23]. Ren et al. [24] also investigated the performances of post heated silicone-based polyurethane/ polymethacrylate membrane constructed by the electrospinning technique [24]. Exceptional breathability results were obtained when evaluating the performances of porous membranes produced by Zhou et al. [23] and Ren et al. [24]. Lv et al. [25] incorporated halloysite nanotubes nanofluids onto polyacrylonitrile porous membranes obtained by the electrospinning technology [25].

Despite the numerous studies devoted to the development of porous membranes, these structures still have some limits such as pores blocking which engender a drop in the membrane breathability and its structure deterioration [26]. To remedy this issue, many researchers tried to modify porous membranes surface chemistry with expensive and arduous methods [26]. Nevertheless, poor adhesion between deposit polymers and membrane surface was reported [26].

Other researchers focused on the development of nonporous membranes. Generally known, these polymer products are polyacrylonitrile based and show low mechanical performances [9]. On the other hand, nonporous materials are almost always produced by the melt extrusion method. However, membranes obtained by this technique have low water vapor permeability [9]. In a study conducted by Gorji et al. [27] a dense membrane was produced with graphene oxide- based nanocomposite hydrogel. The obtained structure with amended breathability was judged suitable for producing protective garments [27].

In this research, a hydrophilic breathable membrane was produced by using a facile technique that does not require expensive equipment. The aim was to obtain an industrializable breathable membrane that could be laminated to other textile layers to enhance their surface hydrophobicity and resistance to water penetration without restricting their breathability.

Experimental

Chemicals and reagents

To produce the dense membrane, the first chemical product (Product (A)) was an aliphatic polyester polyurethane copolymer dispersion, namely Appretan® N5122 liq. The second one (Product (B)), namely Appretan® N92101 liq was an acrylic ester copolymer dispersion. A thickener (Lutexal CSN liq) was also used. All products were supplied from Archroma, Spain.

Polymeric membrane preparation

To obtain membranes with uniform thicknesses a Werner Mathis laboratory coating machine type AG (Oberhasi, Switzerland) was utilized. This machine is composed essentially of two compartments; a coating head and an oven. The coating head consists of a roller and a blade. The position of the blade can be adjusted by varying its height and the angle that it forms with the horizontal plan. The blade height can be adjusted to an accuracy of 0.01 mm by the aim of clock gauges. To obtain the polymeric membrane the blade was fixed at position four (this parameter defines the angle that forms the blade with the horizontal plan) and its height was adjusted at 0.8 mm. The membrane preparation process is presented in Figure 1.

Experimental design

The main parameters that can affect the membrane hydrophilicity are its thickness, the quantities of the two used products, and the polymer blend viscosity. For hydrophilic membranes, the lower is the thickness, the higher is the water vapor transmission rate [2,28].

In this research, it was not possible to obtain membranes with a blade height less than 0.8 mm. The total thickness (thickness of the release fabric and of the paste layer) was equal to 0.8 mm. The viscosity of the polymeric paste was fixed in a way to obtain a homogenous even layer. For each set of experiments, the thickener quantity was determined so that the same viscosity could be obtained for all prepared pastes. The viscosity of the prepared polymer blend was controlled by using a Brookfield DV-I viscometer (Massachusetts, USA). The viscosity mean value was fixed at 80000 Pa·s. The chosen viscosity value ensures the obtention of a polymeric paste that can be easily spread on the release textile fabric. Based on pre-tests, drying temperature and time were set at 115°C and 3 min, respectively. For the crosslinking time it was fixed at 3 min. The

crosslinking temperature was specified by the products supplier and was equal to 165°C. Dried and cured membranes were then removed from the textile carrier.

As a pre-test, a first membrane was prepared only with acrylic ester copolymer (Product (B)). The composition was 60 mL of distilled water and 40 g of acrylic ester copolymer. The paste viscosity was adjusted and fixed at 80000 Pa·s by adding 1.8 g of thickener. The water vapor permeability of the obtained membrane was of 399.493 $g \cdot m^{-2} \cdot day^{-1}$. In order to enhance the membrane breathability, polyester polyurethane dispersion was added to the mixture. Both product quantities were chosen and fixed based on pre-tests. The lowest and the highest quantities for products (A) and (B) were determined in a way to obtain a breathable membrane that can be easily removed from the siliconized textile career.

To study effects of both used chemical products on the obtained membrane breathability, a general full factorial design was used. This design accommodates factors with more than two levels. For statistical analysis, Tests significance level (α) was fixed at 10% which means that factors with p-values lower than 0.1 were considered significant. Factors that might have an influence on the obtained membrane breathability were studied. These factors were polyester polyurethane copolymer and acrylic ester copolymer quantities. Studied factors and corresponding levels are recapitulated in Table 1.

Table 1

Using the Minitab 18 statistical software nine experiments were generated. Each experiment set was carried out three times. To evaluate the breathability of produced membranes, two responses were analyzed. These responses were the water vapor permeability index (WVPI (%)) and the absorption rate (Abs rate (%)). Effects of both used products on the studied responses were evaluated by using ANOVA analysis tool. Factors and interactions with p-values equal to 0 were considered highly significant and those with p-values less or equal to 0.1 were considered significant. Optimum sets for inputs that give the highest absorption rate (%) and water vapor permeability index (%) values were also determined.

Absorption rate determination

To evaluate the absorption rates membrane square samples with an area equal to 25 cm^2 were weighed and impregnated in 100 mL of distilled water for 30 minutes then

drained for 5 minutes. Samples were then re-weighed and absorption rate values were determined by using equation (1) [29]:

$$Abs\ Rate\ (\%) = \frac{M_f - M_i}{M_i} \times 100 \quad (1)$$

Where Abs Rate (%) is the membrane absorption rate, M_f (g) is the membrane mass after 30 minutes in distilled water and 5 minutes of draining time, and M_i (g) is the dry membrane mass.

Water vapor permeability index determination

To avoid discomfort feeling, perspiration should be evacuated from the skin to the surrounded atmosphere. Actually, a high water vapor permeability of a cloth assures a comfort sensation to the wearer. On the other hand, the fabric water vapor permeability (WVP) can be defined as the mass of water vapor that is transported through a unit area of a fabric in a defined period of time [30–33].

To evaluate breathability of produced membranes, a water vapor permeability apparatus type M261 (SDL Atlas, Rock Hill, USA) was used and WVPs ($g{\cdot}m^{-2}{\cdot}day^{-1}$) were determined as specified in the BS 7290:1990 standard and calculated by referring to equation (1) [34].

$$WVP\ (g{\cdot}m^{-2}{\cdot}day^{-1}) = \frac{24 \times M_{loss}}{A \times t} \quad (1)$$

Where M_{loss} (g) is the assembly (dish filled with distilled water, support, cover ring, and test membrane) mass loss after the testing period, A (m^2) is the exposed test membrane area, and t (h) is the testing time.

To eliminate errors due to conditioning a dense cellophane membrane, which was supplied from Measurement Technology Northwest, USA was used as a reference. The WVP of the reference membrane was determined and was equal to 1344 $g{\cdot}m^{-2}{\cdot}day^{-1}$. The water vapor permeability indexes (WVPIs (%)) for prepared membranes were then deduced by using equation (2) [34].

$$WVPI\ (\%) = \frac{WVP_{membrane}}{WVP_{reference}} \times 100 \quad (2)$$

Where $WVP_{membrane}$ ($g{\cdot}m^{-2}{\cdot}day^{-1}$) is the water vapor permeability of the produced membrane and $WVP_{reference}$ ($g{\cdot}m^{-2}{\cdot}day^{-1}$) is the water vapor permeability of the reference cellophane membrane.

Surface free energy determination

The surface free energy of the optimal membrane was determined by referring to the Owens-Wendt-Rabel-Kaelble (OWRK) method. For this purpose, water (polar liquid) and diiodomethane solution (non-polar solution) were used. The wettability of the obtained product was evaluated by measuring contact angles that forms each liquid with the dense membrane surface. For each liquid, an equation relating the membrane surface free energy polar and dispersive components to the contact angle was established (equation (3)) [35,36].

$$\gamma_L \times (1 + cos\theta_L) = 2\sqrt{\gamma_{dS}\gamma_{dL}} + 2\sqrt{\gamma_{pS}\gamma_{pL}} \quad (3)$$

Where γ_L (mN·m^{-1}) is the used liquid surface tension, θ_L (°) is the measured contact angle, γ_{dS} and γ_{pS} (mN·m^{-1}) are respectively dispersive and polar components of the membrane surface free energy, and γ_{dL} and γ_{pL} (mN·m^{-1}) are respectively dispersive and polar components of the used liquid surface tension.

The resolution of the obtained two equations system and the determination of γ_{dS} and γ_{pS} (mN·m^{-1}) enable us to calculate their sum which corresponds to the surface free energy of the produced optimal membrane [35,36].

Membrane morphology analysis

The polymeric membrane external morphology was analyzed with a scanning electron microscope type Jeol, JSM-5400. Applied voltage for sample scanning was equal to 15 kV. Front and back sides as well as the section view of the membrane were captured with magnifications ranging from 50 to 350×.

Results and Discussions

Study of the absorption rate

To prevent uncomfortable feeling resulting from transpiration accumulation, the water absorption rates of the produced membranes were measured. A general full factorial design was used to evaluate effects of both used products on the Abs rate (%) response. Absorption rate values (%) of prepared membranes are recapitulated in Table 2.

Table 2

Using the adjusted sum of squares for tests, the analysis of variance for the absorption rate response was elaborated and generated by the Minitab 18 software.

Results from the two-way ANOVA analysis showed that product (B) had a significant effect on the studied response with a p-value lower then 0.1 (p-value = 0.059) and an adjusted sum of squares (Adj SS) equal to 338.06. The effect of product (A) was judged not significant (p-value = 0.583> 0.1).

The main effects plot for the absorption rate is represented in Figure 2(a). It was found that the quantities of products (A) and (B) had a negative effect on the absorption rate response.

Figure 2

For product (B) this effect was highly significant with a plotted line that was very steep from the x-axis. On average, when product (B) quantity was varied from 40 to 60 g, a decrease on the absorption rate percentage was noticed. Water absorption was influenced by the polymeric membrane composition. The variation of product (B) quantity had the most important effect on the mean absorption rate value. It is true that an augmentation in product (B) quantity heightened the presence of hydrophilic sites (-O-) coming from the acrylic ester copolymer chains (Figure 3), however, a high concentration of this product exhibited the water absorption rate since it restricted chain inter-spaces and decreased the interactions between the hydrophilic groups of polymer chains and water molecules. Also, there are hydrophobic sites on the backbone chains of the acrylic ester copolymer. The presence of these sites also affected negatively the absorption rate. This explains the decrease in water absorption rate values when product (B) quantity was increased.

Figure 3

On the other hand, when product (A) quantity was varied from 8 to 12 g the absorption rate increased. Yet, this augmentation is not really important since the plotted line relating the two mean values for both categories is almost parallel to the x-axis. Added to that, a decrease in absorption rate values was noticed when this product quantity was varied from 12 to 16 g. The interpretation made when varying product (B) quantity remains valid in this case.

Study of the water permeability index

The WVPI values (%) were measured for all prepared membranes. Obtained results are recapitulated in Table 3.

Table 3

The analysis of variance for the WVPI response was elaborated by using the adjusted sum of squares for tests. After ANOVA analyzing it was noticed that both studied products had a significant effect on the WVPI (%) with p-values lower than 0.1. Actually, p-values were equal to 0.082 and 0.093, respectively for products (A) and (B). It was concluded that product (A) had the most significant effect on the studied response with the lowest p-value and the highest adjusted sum of squares (Adj SS equal to 137.73 and 126.3 for products (A) and (B), respectively).

From the main effects plot of the WVPI (%) presented in Figure 2(b) it can be noticed that as well as the quantity of product (A) increased there was an increase in the WVPI (%). For hydrophilic membranes the water vapor permeability is governed by chemical interactions between polymer hydrophilic sites (Figure 3) and water vapor molecules. The rise in the water vapor permeability when increasing product (A) quantity was the result of the increase in the number of sites that are able to interact with water vapor molecules. In addition, the membrane thickness and the concentration of water vapor adsorbed and absorbed in the membrane polymeric matrix had an effect on its water vapor transmission rate. As well as the thickness of the membrane increased, its water vapor permeability decreased.

Generally known, polyurethanes are hydrophobic [15]. On the other hand, for non-homogenous polymeric systems the diffusion rate of water vapor molecules depends of their concentration in the membrane. The diffusion of water vapor molecules through the membrane can be described by Fick's second law [2].

Apart from this, considering that product (A) is a polyester polyurethane dispersion and that polyester polyurethane copolymer is not soluble in aqueous solution, hydrophilic segments are generally incorporated in its chain to make it dispersible in water.

In this research, polymeric membranes with the same thickness were produced. When the quantity of product (A) was increased the amount of hydrophilic sites in the membrane was enhanced. As a result, the water vapor content on the membrane increased. Based on Fick's second law, the diffusion rate also rose. As a consequence, an augmentation on the water vapor permeability index was noticed.

For quantities of product (B) varying from 40 to 50 g, the WVPI (%) decreased. This is due to the restriction of the free volume in the polymeric matrix. Higher interactions between polymeric chains made amorphous region gaps and chain interspaces smaller which blocked the water vapor passage.

Optimization of the polymeric membrane formulation

To produce a membrane with the best performance in term of breathability, a general full factorial design was used. Two factors that are the quantities of aliphatic polyester polyurethane (product (A)) and acrylic ester (product (B)) copolymers were studied. Analyzed and optimized responses were the absorption rate (%) and the water vapor permeability index (%). The set target was to maximize both studied responses in order to obtain a nonporous membrane with the highest performances in terms of water vapor permeability and absorption rate. The obtained optimized values are shown in Figure 4.

Figure 4

Predicted optimized values for the absorption rate (%) and the water vapor permeability index (%) were equal to 47.158 (d=0.795) and 42.105% (d=1), respectively. The composite desirability (D) was of 0.89. This value was close to the unit meaning that obtained responses satisfied the set goals. The best performances in terms of absorption rate (%) and water vapor permeability index (%) were obtained with 16 and 40 g of product (A) and product (B), respectively. Based on obtained results, the optimal membrane was judged breathable.

The surface free energy (SFE ($mN.m^{-1}$)) of the membrane produced with the optimized formulation was also determined by referring to the Owens-Wendt method [35,36]. Contacts angles (Θ_{water}) and ($\Theta_{diiodomethane}$) were measured with distilled water and diiodomethane solution. Obtained results are shown in Table 4.

Table 4

In a previous study done by Ghezal et al. [37], other physical characteristics of the optimal membrane such as the mass per unit area and the thickness were determined [37]. Ghezal et al. [37] also tested the air permeability ($L \cdot m^{-2} \cdot s^{-1}$) and the resistance to water penetration (RWP (Schmerber)) of the developed optimal membrane. They concluded that the membrane windproofness resulted from the absence of pores in the produced polymeric structure [37].

The external morphology of the produced dense membrane was also investigated. Front and back sides as well as the section view of the polymeric structure are shown in Figure 5.

Figure 5

The membrane side which was in direct contact with the siliconized textile fabric (Figure 5(b)) was smoother than its front side which presented some irregularities (Figure 5(a)).

Micrographs of the obtained membrane (Figures 5(a), (b), and (c)) displayed blind micropores. The produced material was considered as a dense nonporous membrane since it contained closed pores. These blind micropores were not resulting from the presence of pore-forming agents nor the release of low-molecular-weight product during polymer materials thermosetting. From Figure 6, we noticed that the obtained blind micropores were of two different morphological types. Actually, these close micropores are not only caused by entrapped air in the paste mixture used for producing the polymer membrane but also the method employed for the polymer mixture spreading on the siliconized textile.

Figure 6

After polymer layer thermosetting, the persistence of the micro foam is the main reason for the appearance of these close micropores in the produced membranes.

Conclusion

The aim of this research was the development of a breathable membrane that can be laminated to textile and non-woven fabrics. Developed membranes were mainly made from aliphatic polyester polyurethane and acrylic ester copolymer dispersions. To optimize the membrane formulation, quantities of polyester polyurethane and acrylic ester copolymer dispersions were varied. Water vapor permeability index (%) and water absorption rate (%) responses were analyzed. For this purpose, a general full factorial design was employed. Effects of studied factors on both studied responses were investigated. Based on obtained results, it was found that Product (B) quantity had the most significant effect on the water absorption rate. Considering obtained p-values it was found that both used products had a significant effect on studied responses.

Determined optimal values of used products were equal to 16 and 40 g, respectively for aliphatic polyester polyurethane and acrylic ester copolymers. Predicted optimized responses were of 47.158% for the absorption rate and 42.105% for the WVPI. Finally, it was concluded that the developed membrane was breathable, windproof, and hydrophobic.

References

[1] M. Zahid, G. Mazzon, A. Athanassiou, I.S. Bayer, Adv. Colloid Interface Sci. 270 (2019) 216–250. https://doi.org/10.1016/j.cis.2019.06.001

[2] A. Gugliuzza, E. Drioli, J. Memb. Sci. 446 (2013) 350–375. https://doi.org/10.1016/j.memsci.2013.07.014

[3] F.J. Maksoud, M. Lameh, S. Fayyad, N. Ismail, A.R. Tehrani-Bagha, N. Ghaddar, K. Ghali, J. Appl. Polym. Sci. 135 (2018) 45660. https://doi.org/10.1002/app.45660

[4] Waterproof Breathable Fabrics Report, Balancing Performance and Environmental sustainability, https://www.innovationintextiles.com/waterproof-breathable-fabrics-balancing-performance-and-environmental-sustainability/ [accessed 2 February 2024].

[5] J. Sheng, Y. Xu, J. Yu, B. Ding, ACS Appl. Mater. Interfaces 9 (2017) 15139–15147. https://doi.org/10.1021/acsami.7b02594

[6] J. Zhao, W. Zhu, X. Wang, L. Liu, J. Yu, B. Ding, ACS Nano 14 (2020) 1045–1054. https://doi.org/10.1021/acsnano.9b08595

[7] F. Fornasiero, Curr. Opin. Chem. Eng. 16 (2017) 1–8. https://doi.org/10.1016/j.coche.2017.02.001

[8] Y. Zhang, X. Li, H. Wang, B. Wang, J. Li, D. Cheng, Y. Lu, Nanomaterials 12 (2022) 3071. https://doi.org/10.3390/nano12173071

[9] Y. Chang, F. Liu, Materials (Basel, Switz) 16 (2023) 5339. https://doi.org/10.3390/ma16155339

[10] S. Shi, Y. Han, J. Hu, Prog. Org. Coat. 137 (2019) 105303. https://doi.org/10.1016/j.porgcoat.2019.105303

[11] D. Negru, L. Buhu, E. Loghin, I. Dulgheriu, A. Buhu, Ind. Text. 68 (2017) 269–274. http://doi.org/10.35530/IT.068.04.1350

[12] S. Shi, C. Zhi, S. Zhang, J. Yang, Y. Si, Y. Jiang, Y. Ming, K.T. Lau, B. Fei, J. Hu, ACS Appl. Mater. Interfaces 14 (2022) 39610–39621. https://doi.org/10.1021/acsami.2c11251

[13] A. Mukhopadhyay, V.K. Midha, J. Ind. Text. 37 (2008) 225–262. https://doi.org/10.1177/1528083707082164

[14] A. Mukhopadhyay, V.K. Vinay Kumar Midha, J. Ind. Text. 38 (2008) 17–41. https://doi.org/10.1177/1528083707082166

[15] M. Gorji, M. Karimi, S. Nasheroahkam, J. Ind. Text. 47 (2018) 1166–1184. https://doi.org/10.1177/1528083716682920

[16] E.-Y. Kim, J.-H. Lee, D.-J. Lee, Y.-H. Lee, J.-H. Lee, H.-D. Kim, J. Appl. Polym. Sci. 129 (2013) 1745–1751. https://doi.org/10.1002/app.38860

[17] L. Sheng, X. Zhang, Z. Ge, Z. Liang, X. Liu, C. Chai, Y. Luo, J. Coat. Technol. Res. 15 (2018) 1283–1292. https://doi.org/10.1007/s11998-018-0096-x

[18] Y. Ma, M. Zhang, W. Du, S. Sun, B. Zhao, Y. Cheng, Polymers (Basel, Switz). 15 (2023) 1759. https://doi.org/10.3390/polym15071759

[19] Y. Guo, W. Zhou, L. Wang, Y. Dong, J. Yu, X. Li, B. Ding, ACS Appl. Bio Mater. 2 (2019) 5949–5956. https://doi.org/10.1021/acsabm.9b00875

[20] Y. Zhang, T.T. Li, H.T. Ren, F. Sun, B.C. Shiu, C.W. Lou, J.H. Lin, J. Sandwich Struct. Mater. 23 (2021) 2817–2831. https://doi.org/10.1177/1099636220909750

[21] W. Zhou, X. Gong, Y. Li, Y. Si, S. Zhang, J. Yu, B. Ding, J. Colloid Interface Sci. 602 (2021) 105–114. https://doi.org/10.1016/j.jcis.2021.05.171

[22] W. Zhou, J. Yu, B. Ding, Compos. Commun. 35 (2022) 101337. https://doi.org/10.1016/j.coco.2022.101337

[23] W. Zhou, X. Gong, Y. Li, Y. Si, S. Zhang, J. Yu, B. Ding, Chem. Eng. J. (Amsterdam, Neth.) 427 (2021) 130925. https://doi.org/10.1016/j.cej.2021.130925

[24] G. Ren, Z. Li, L. Tian, D. Lu, Y. Jin, Y. Zhang, B. Li, H. Yu, HeJianxin, D. Sun, Colloids Surf., A 658 (2023) 130643. https://doi.org/10.1016/j.colsurfa.2022.130643

[25] Y. Lv, X. Sun, S. Yan, S. Xiong, L. Wang, H. Wang, S. Yang, X. Yin, Compos. Commun. 33 (2022) 101211. https://doi.org/10.1016/j.coco.2022.101211

[26] A. Saffar, P.J. Carreau, A. Ajji, M. R.Kamal, J. Membr. Sci. 462 (2014) 50–61. https://doi.org/10.1016/j.memsci.2014.03.024

[27] M. Gorji, M. Karimi, G. Mashaiekhi, S. Ramazani, Polym.-Plast. Technol. Mater. 58 (2019) 182–192. https://doi.org/10.1080/03602559.2018.1466174

[28] K.T. Djoko, H. Hadiyanto, D. Deariska, L. Nugraha, Chem. Ind. Chem. Eng. Q. 24 (2018) 139–147. https://doi.org/10.2298/CICEQ170112026K

[29] Z. Li, X. Yue, G. He, Z. Li, Y. Yin, M. Gang, M. Gang, M. Gang, Z. Jiang, Int. J. Hydrogen Energy 40 (2015) 8398–8406. https://doi.org/10.1016/j.ijhydene.2015.04.138

[30] B. Das, A. Das, V.K. Kothari, R. Fanguiero, M. de Araújo, Autex Res. J. 7 (2007) 100–

110. https://doi.org/10.1515/aut-2007-070204

[31] B. Das, A. Das, V.K. Kothari, R. Fangueiro, M. de Araújo, Autex Res. J. 7 (2007) 194–216. https://doi.org/10.1515/aut-2007-070305

[32] A. Razzaque, P. Tesinova, L. Hes, J. Salacova, H.A. Abid, Fibers Polym. 18 (2017) 1924–1930. https://doi.org/10.1007/s12221-017-1154-1

[33] J. Huang, Text. Res. J. 86 (2016) 325–336. https://doi.org/10.1177/0040517515588269

[34] The British Standards Institution, BS 7209:Water Vapor Permeable Apparel Fabrics (1990). https://knowledge.bsigroup.com/products/specification-for-water-vapour-permeable-apparel-fabrics/standard

[35] A. Rudawska, E. Jacniacka, Int. J. Adhes. Adhes. 29 (2009) 451–457. https://doi.org/10.1016/j.ijadhadh.2008.09.008

[36] Lefebvre, G. (2011). [Ph.D. Thesis, University of Toulouse]. HAL Open Science. https://theses.hal.science/tel-04274825/document

[37] I. Ghezal, A. Moussa, I. Ben Marzoug, A. El-Achari, C. Campagne, F. Sakli, Chem. Ind. Chem. Eng. Q. (2023). https://doi.org/10.2298/CICEQ230407029G

Figure captions

Figure 1. Membrane preparation process.

Figure 2. Main effects plots (data means) for: (a) Abs rate (%) and (b) WVPI (%) of the studied polymeric membrane.

Figure 3. FT-IR spectrum of the membrane produced with polyurethane polyester and acrylic ester copolymer dispersions (Product A: polyester polyurethane copolymer; Product B: acrylic ester copolymer).

Figure 4. Polymeric membrane formulation optimization.

Figure 5. Scanning electron microscope image of the dense membrane (aliphatic polyester polyurethane dispersion: 16 g; acrylic ester copolymer dispersion: 40 g): (a) front side, (b) back side, and (c): section view.

Figure 6. Scanning electron microscope image of air bubbles in the dense membrane (aliphatic polyester polyurethane dispersion (product A): 16 g; acrylic ester copolymer dispersion (product B): 40 g); (a, b) front views and (b, c) back views.

Tables

Table 1. Studied factors and corresponding levels.

Factors	Factor Codes	Variation Levels		
		Level 1	Level 2	Level 3
Product A quantity (g)	A	8	12	16
Product B quantity (g)	B	40	50	60

Product A: aliphatic polyester polyurethane dispersion.

Product B: acrylic ester copolymer dispersion.

Table 2. Absorption rate values for the different prepared membranes.

Exp. N°	Factors		Thickener quantity (g)	Abs rate (%)	
	Product A (g)	Product B (g)		Mean values (%)	Coefficient of variation (%)
1	8	40	2.0	45.992	4.447
2	8	50	2.60	45.142	1.564
3	8	60	3.04	38.790	6.093
4	12	40	2.50	51.229	3.740
5	12	50	2.92	40.770	1.890
6	12	60	2.95	39.080	2.292
7	16	40	2.70	52.401	4.642
8	16	50	2.85	39.096	1.342
9	16	60	3.50	26.782	3.671

The absorption rate mean values (Abs rate (%)) are the average of three different measurements.

Table 3. WVPI (%) values for the different prepared membranes.

Exp. N°	Factors		WVPI (%)	
	Product A (g)	Product B (g)	Mean values (%)	CV (%)
1	8	40	34.478	2.073
2	8	50	21.239	0.685
3	8	60	30.747	3.438
4	12	40	38.139	1.453
5	12	50	25.806	4.73
6	12	60	31.778	2.81
7	16	40	37.510	1.283
8	16	50	36.787	4.7
9	16	60	40.715	4.35

The water vapor permeability index mean values (WVPI (%)) are the average of three different measurements.

Table 4. Optimal membrane characteristics.

Characteristics	Values
Thickness [37]	293 µm ± 2.449 %
Mass per unit area [37]	152.96 $g \cdot m^{-2}$ ± 2.875 %
Θ_{water}	66° ± 8.557%
$\Theta_{diiodomethane}$	34° ± 8.98%
SFE	39.234 $mN \cdot m^{-1}$
WVPI	37.510% ± 1.283%
Absorption rate	52.401% ± 4.642%
Air permeability [37]	0 $L \cdot m^{-2} \cdot s^{-1}$
RWP [37]	88.26 Schmerber ± 1.6%

Θ_{water} (°) and $\Theta_{diiodomethane}$ (°) are contact angles measured respectively with distilled water and diiodomethane solution, WVP ($g \cdot m^{-2} \cdot day^{-1}$) and WVPI (%) are respectively the water vapor permeability and the water vapor permeability index, and RWP (Schmerber) is the resistance to water penetration.

Figures

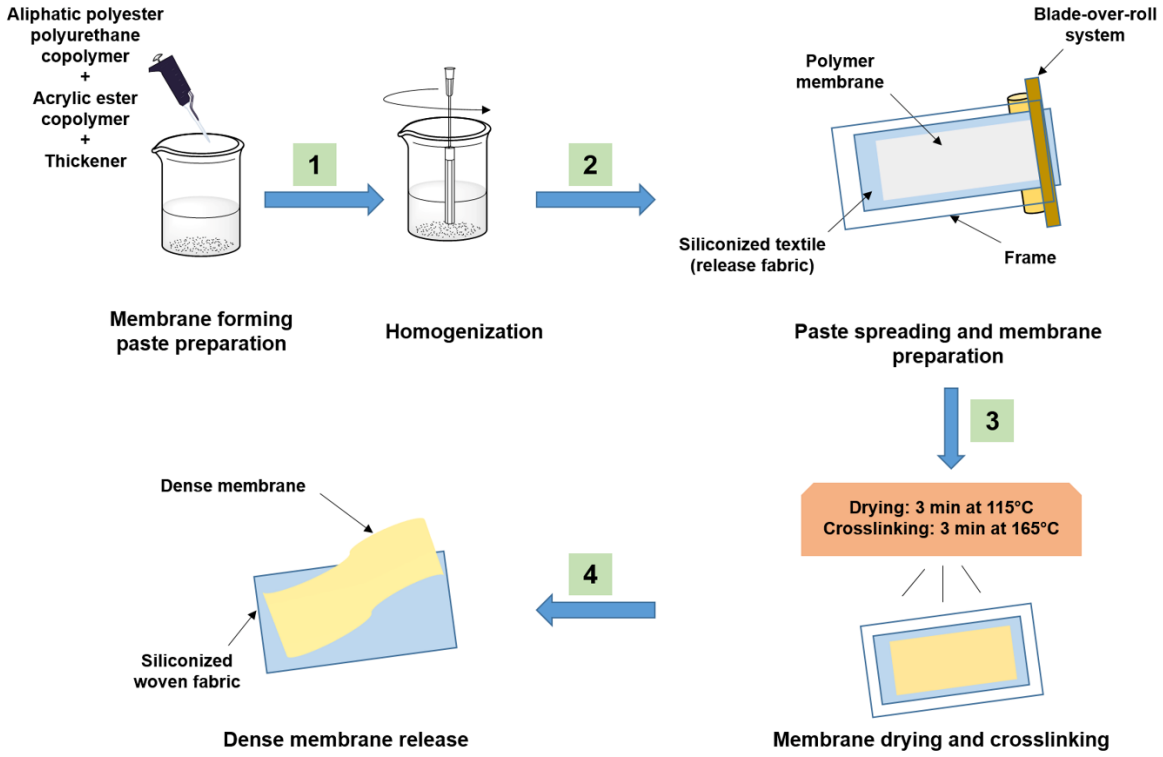

Figure 1

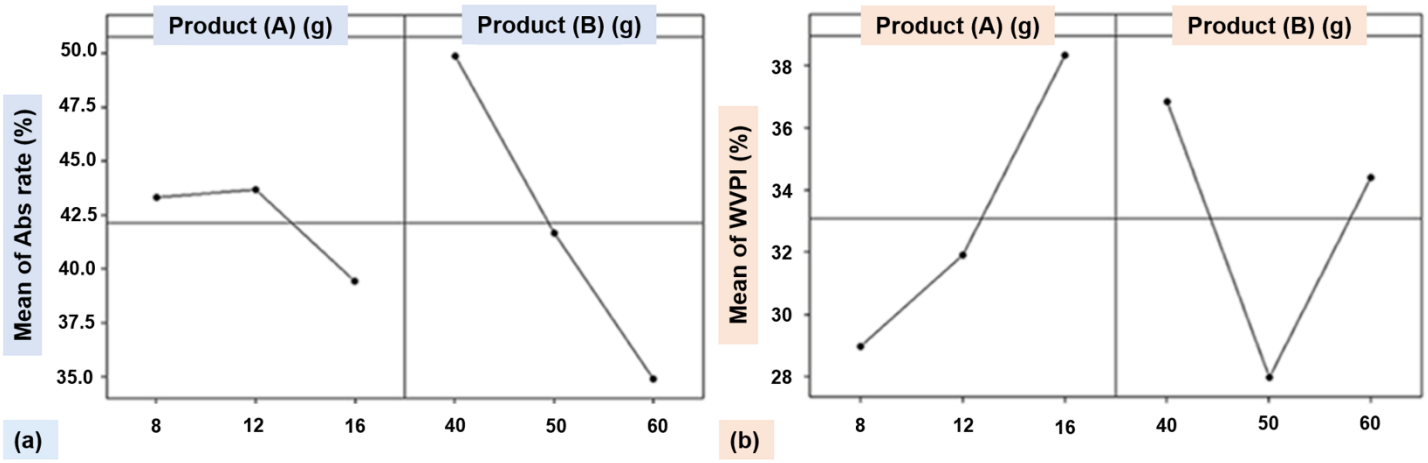
Product (A) (g)
Product (B) (g)
Mean of Abs rate (%)
50.0
47.5
45.0
42.5
40.0
37.5
35.0
8
12
16
40
50
60
(a)
Product (A) (g)
Product (B) (g)
Mean of WVPI (%)
38
36
34
32
30
28
8
12
16
40
50
60
(b)

Figure 2

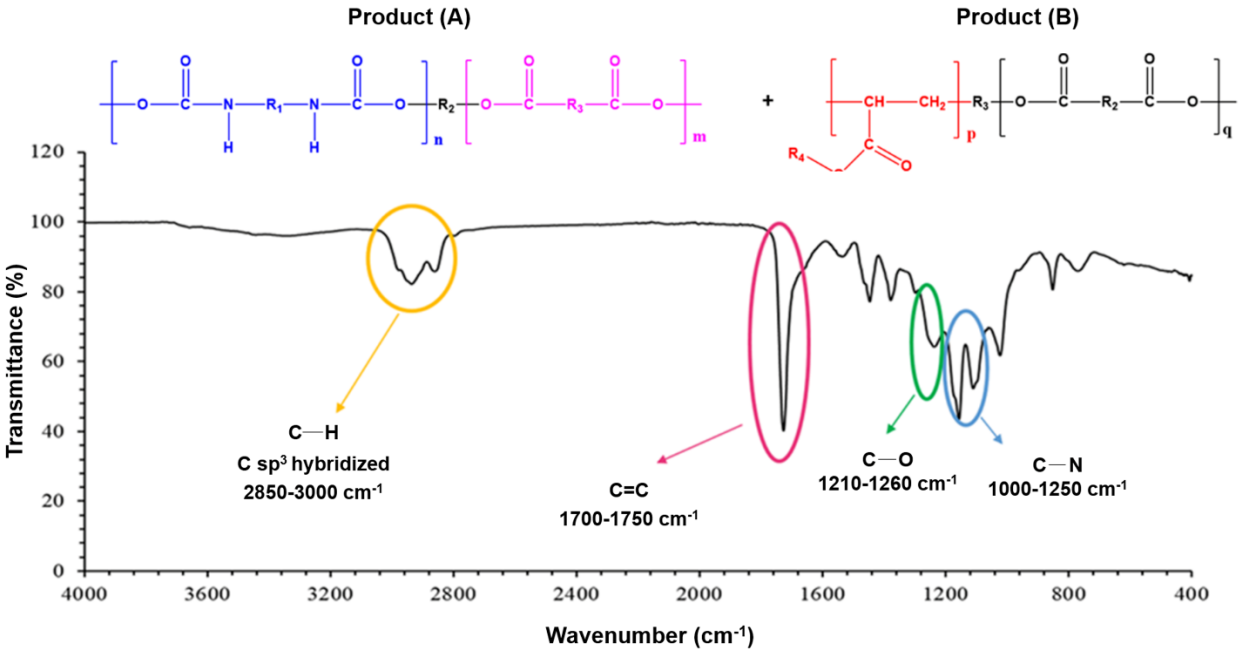
Product (A)
Product (B)
Transmittance (%)
Wavenumber (cm-1)
C—H
C sp3 hybridized
2850-3000 cm-1
C=C
1700-1750 cm-1
C—O
1210-1260 cm-1
C—N
1000-1250 cm-1

Figure 3

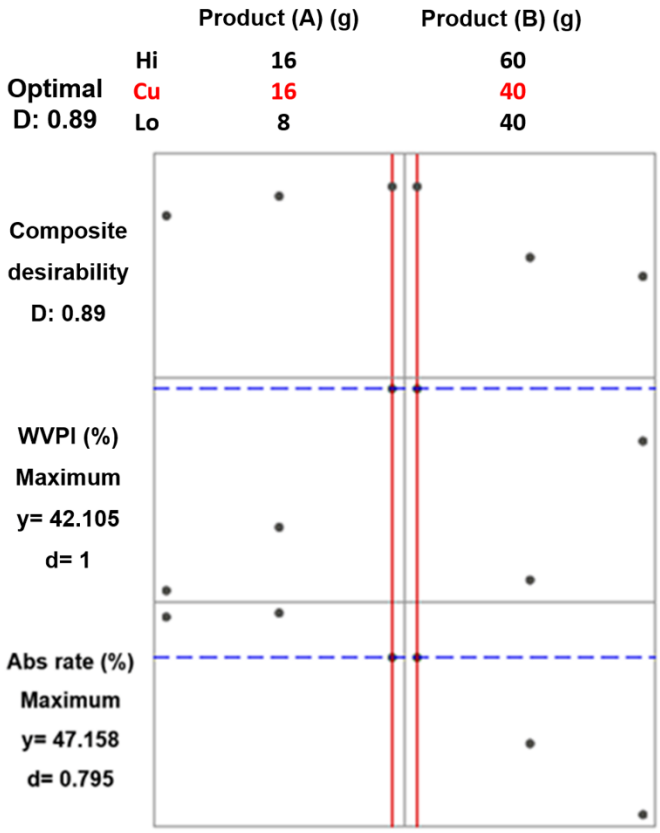
Product (A) (g)
Product (B) (g)
Hi
16
60
Optimal
Cu
16
40
D: 0.89
Lo
8
40
Composite
desirability
D: 0.89
WVPI (%)
Maximum
y= 42.105
d= 1
Abs rate (%)
Maximum
y= 47.158
d= 0.795

Figure 4

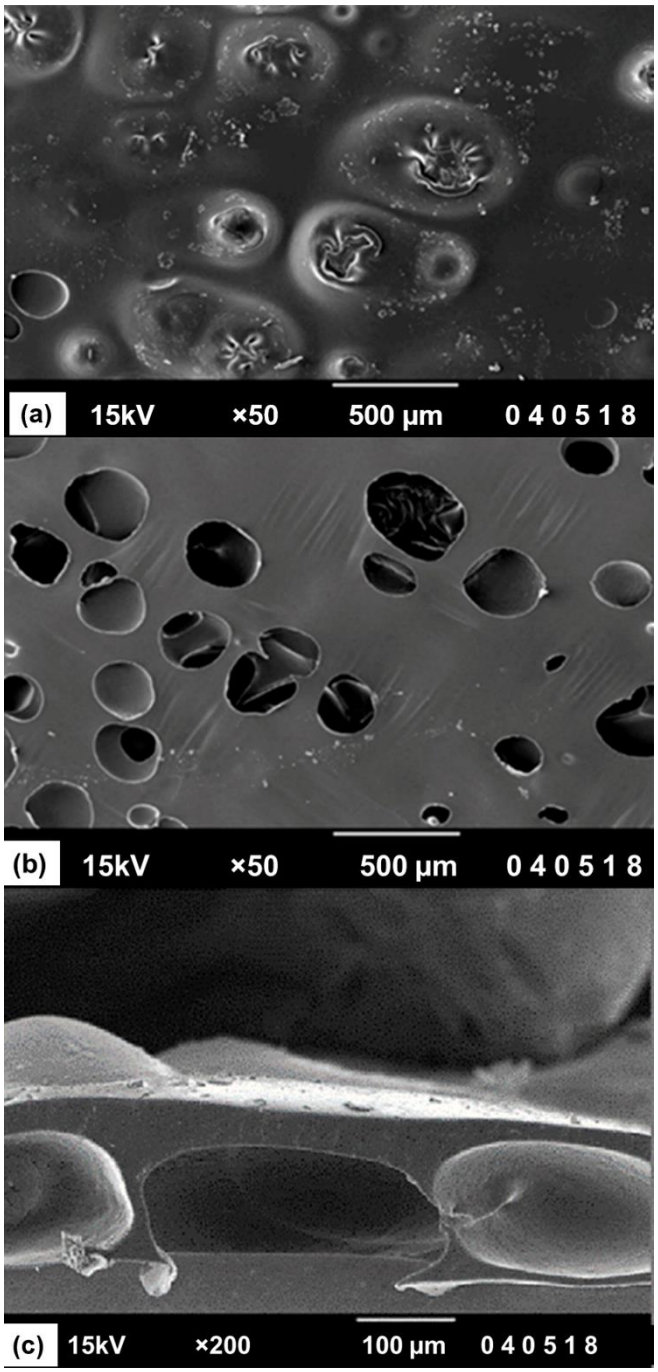
(a) 15kV ×50 500 µm 0 4 0 5 1 8
(b) 15kV ×50 500 µm 0 4 0 5 1 8
(c) 15kV ×200 100 µm 0 4 0 5 1 8

Figure 5

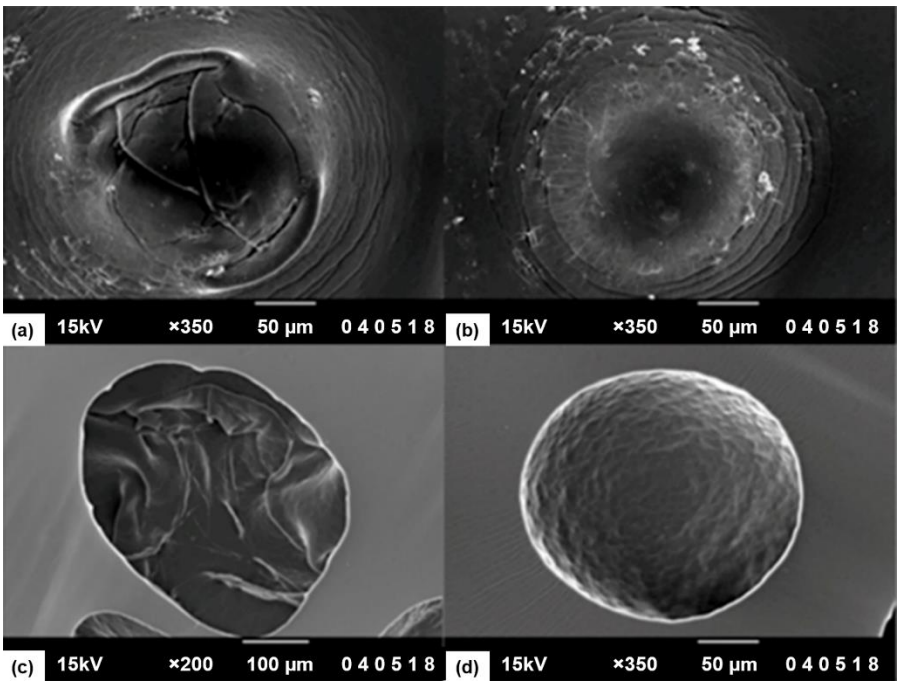
(a) 15kV ×350 50 µm 0 4 0 5 1 8
(b) 15kV ×350 50 µm 0 4 0 5 1 8
(c) 15kV ×200 100 µm 0 4 0 5 1 8
(d) 15kV ×350 50 µm 0 4 0 5 1 8

Figure 6